Cell Reports, Volume *36*

Supplemental information

Regulation of NMDA receptor trafficking and gating by activity-dependent CaMKIIα phosphorylation of the GluN2A subunit

Xuan Ling Hilary Yong, Lingrui Zhang, Liming Yang, Xiumin Chen, Jing Zhi Anson Tan, Xiaojun Yu, Mintu Chandra, Emma Livingstone, Jocelyn Widagdo, Marta M. Vieira, Katherine W. Roche, Joseph W. Lynch, Angelo Keramidas, Brett M. Collins, and Victor Anggono

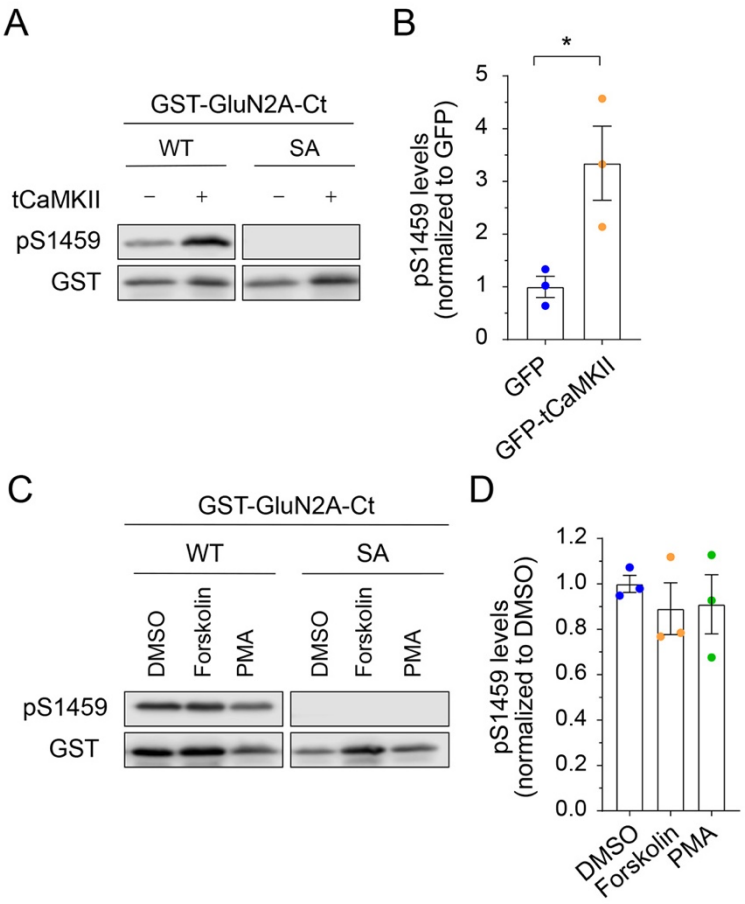

Figure S1 (related to Figure 1). CaMKIIα phosphorylates GluN2A on Ser-1459

(A) HEK293T cells were transfected with pCIS-GluN2A-C-terminal domain (WT or S1459A) and pEGFP or pEGFP-tCaMKIIα (constitutively active truncated CaMKIIα), lyzed and pulled-down with GSH-sepharose. Bound proteins were eluted and resolved by SDS-PAGE, and analyzed by western blotting with specific antibodies against GluN2A pS1459 and GST.

(B) Quantification of Ser-1459 phosphorylation levels after normalizing to GST. Data represent mean ± SEM of band intensities normalized to control values of cells expressing GFP (n = 3). *P < 0.05 using unpaired t-test.

(C) HEK293T cells expressing GST-GluN2A-C-terminal domain (WT or S1459A) were treated with 10 μM forskolin, 1 μM PMA or DMSO (vehicle) for 10 min prior to lysis. Cell lysates were analyzed by immunoblotting with specific antibodies against GluN2A pS1459 and GST.

(D) Quantification of Ser-1459 phosphorylation levels after normalizing to GST. Data represent mean ± SEM of band intensities normalized to control values of vehicle-treated cells (n = 3). No statistical difference was observed among groups as determined by one-way ANOVA.

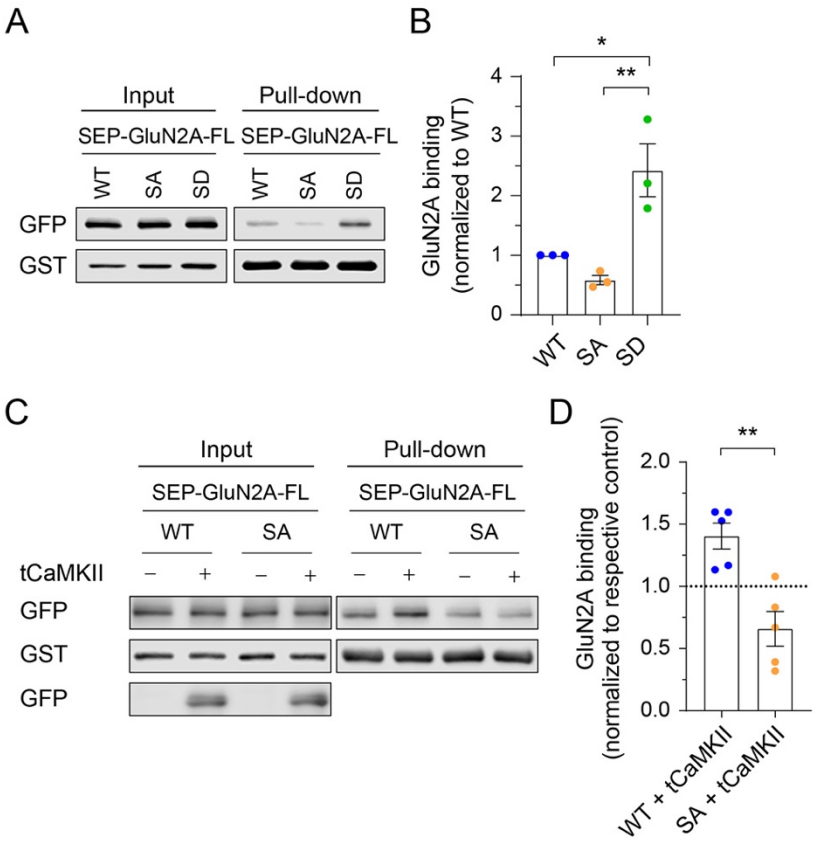

Figure S2 (related to Figure 2). GluN2A phosphorylation on Ser-1459 enhances SNX27 binding

(A) HEK293T cells were co-transfected with plasmids encoding GST-SNX27, GluN1 and full-length SEP-GluN2A (WT, S1459A or S1459D), lyzed and pulled-down with GSH-sepharose. Bound proteins were eluted and resolved by SDS-PAGE, and analyzed by western blotting with specific antibodies against GFP and GST.

(B) Quantification of the level of SEP-GluN2A binding to GST-SNX27. Data represent mean ± SEM of band intensities normalized to control values of cells expressing SEP-GluN2A WT (n = 3). *P < 0.05, **P < 0.01 using one-way ANOVA with Tukey's multiple comparisons test.

(C) HEK293T cells were co-transfected with plasmids encoding GST-SNX27, GluN1 and SEP-GluN2A (WT or S1459A), with pEGFP or pEGFP-tCaMKIIα. Cells were lyzed and pulled-down with GSH-sepharose. Bound proteins and total lysates were analyzed by immunoblotting with specific antibodies against GFP and GST.

(D) Quantification of the level of SEP-GluN2A binding to GST-SNX27. Data represent mean ± SEM of band intensities normalized to the respective control values of cells that expressed GFP only (n = 5). **P < 0.01 using Mann-Whitney test.

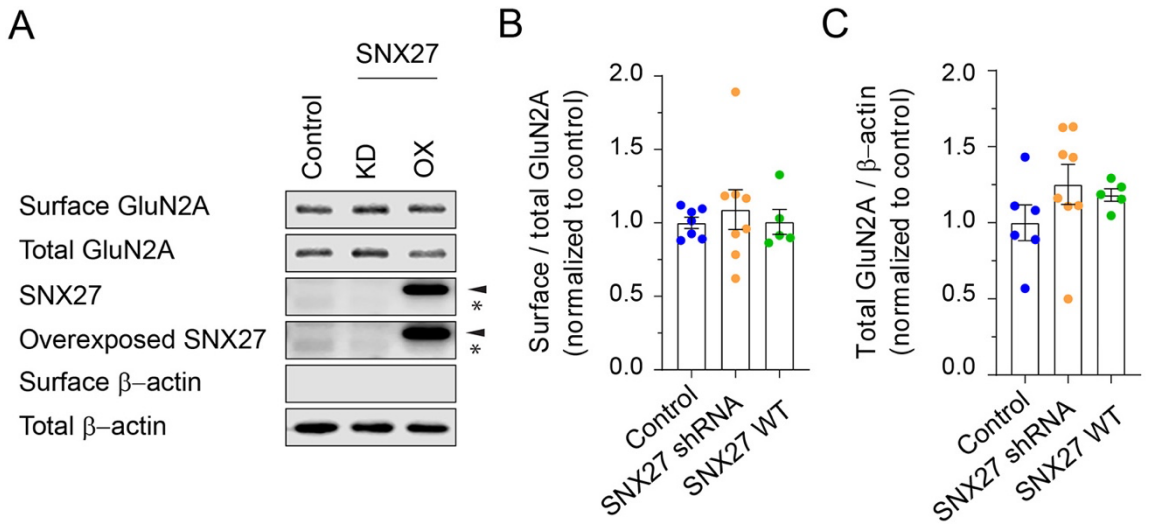

Figure S3 (related to Figure 3). SNX27 does not regulate GluN2A surface expression under basal conditions

(A) Cultured cortical neurons were transduced with lentiviral particles expressing GFP (control), SNX27 shRNA or myc-SNX27 cDNA (OX) at DIV 9. At DIV15, neurons were subjected to surface biotinylation assays. The relative amount of surface and total GluN2A was assessed by western blotting using specific antibodies against GluN2A. SNX27 blots confirmed the levels of knockdown and overexpression. Endogenous and overexpressed SNX27 are indicated by asterisks and arrowheads, respectively.

(B and C) Quantification of the surface/total ratio (B) and total (C) GluN2A after normalizing against β-actin. Data represent mean ± SEM of band intensities normalized to control values of neurons expressing GFP only (*n* = 5-8). No statistical difference was observed among groups as determined by one-way ANOVA.

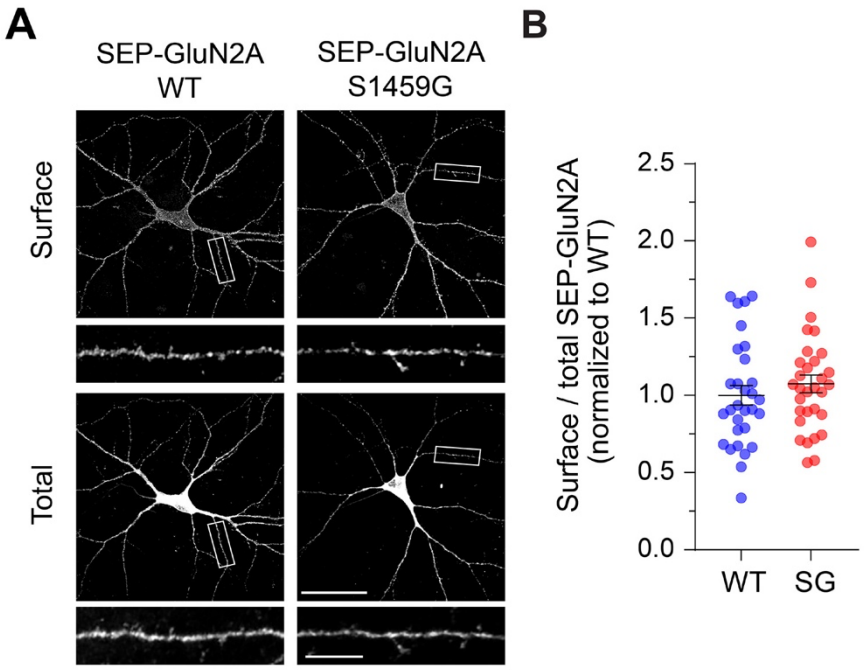

Figure S4 (related to Figure 5). GluN2A S1459G variant does not regulate GluN2A surface expression under basal conditions.

(A) Primary hippocampal neurons were transfected with plasmids encoding SEP-GluN2A, either WT or the phospho-variant S1459G (SG) mutant at DIV12. Representative images of surface and total SEP-GluN2A in a neuron from each group, together with enlarged images of the boxed regions. Scale bars, 50 μm and 10 μm (enlarged images).

(B) Quantification of the surface/total GluN2A ratio normalized to the value of control neurons expressing SEP-GluN2A WT. Data are presented as mean ± SEM (WT, *n* = 30 neurons and S1459G, *n* = 31; from 2 independent cultures).

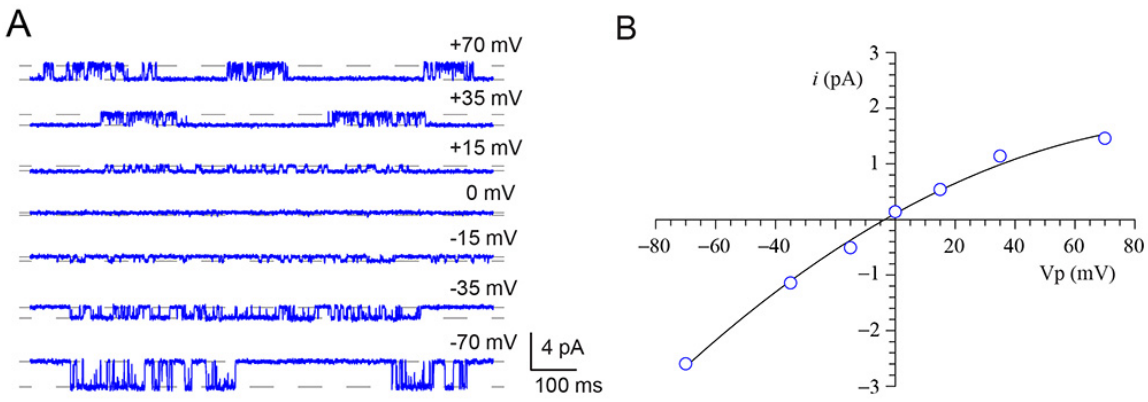

Figure S5 (related to Figure 6). Single channel I-V relationships

(A) Single channel current amplitude as a function of voltage mediated by wild-type GluN1/2A receptors from a single excised patch of membrane. Single receptor currents were elicited by continuously perfusing the recorded patch with 1 mM glutamate, 0 Mg^{2+} and 100 μM glycine at the indicated applied voltages.

(B) The current-voltage (I-V) curve.

Table S1 (related to Figure 2). ITC binding data for SNX27 association with GluN2A C-terminal peptides

Peptide	Sequence	Kd, μM	Δ*H*, kcal/mol	TΔ*S*, kcal/mol	Δ*G*, kcal/mol	N, stoichiometry
WT	YKKMPSIESDV	46.0 ± 2.6	-5.8 ± 1.9	-0.13 ± 0.02	-5.9 ± 1.0	1.2 ± 0.1
S1459A	YKKMPAIESDV	49.9 ± 1.3	-5.3 ± 1.2	0.53 ± 0.03	-5.9 ± 0.9	1.1 ± 0.1
S1459E	YKKMPEIESDV	25.0 ± 2.1	-17.1 ± 1.6	-10.88 ± 1.02	-6.2 ± 0.4	0.9 ± 0.1
S1462E	YKKMPSIEEDV	n.b.d.	n.b.d.	n.b.d.	n.b.d.	n.b.d.
p-S1459	YKKMP(pS)IESDV	13.7 ± 0.7	-9.0 ± 1.0	-2.2 ± 0.9	-6.6 ± 0.03	0.7 ± 0.1

All experiments were performed 3 times. Data are presented as mean ± SD. n.b.d. = no binding detectable.

Table S2 (related to Figure 6). Single channel conductance at -70 mV

Receptor	Conductance, pS
GluN1/GluN2A^{WT}	41.5
GluN1/GluN2A^{S1459G}	42.7
GluN1/GluN2A^{S1459D}	42.7

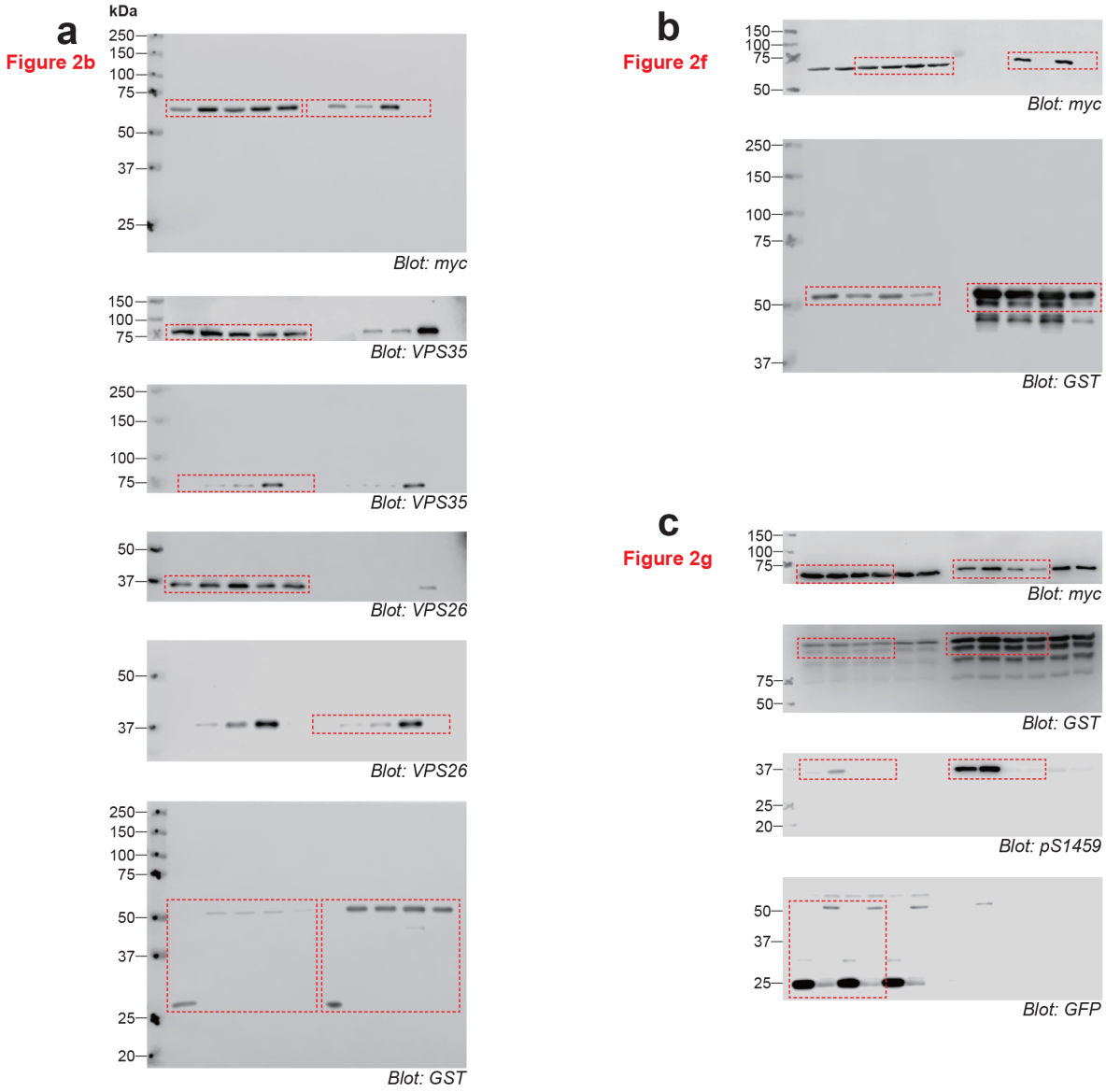

Data S1. Uncropped Images of Western Blots, Related to Figure 2.

Figure 3c

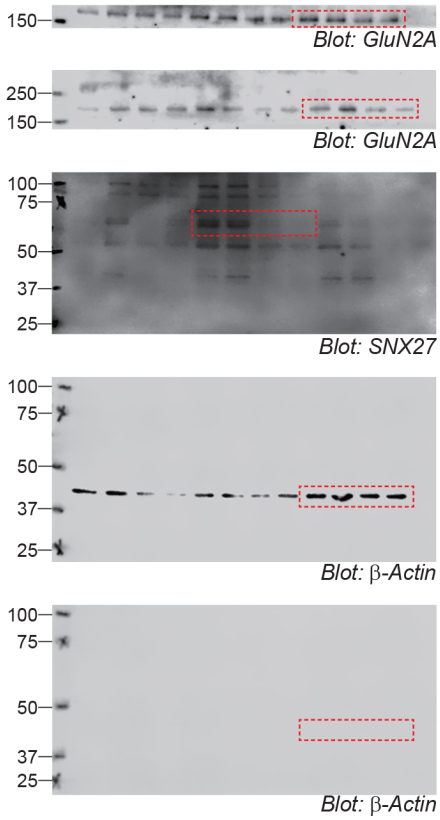

Data S2. Uncropped Images of Western Blots, Related to Figure 3.

Figure 4a

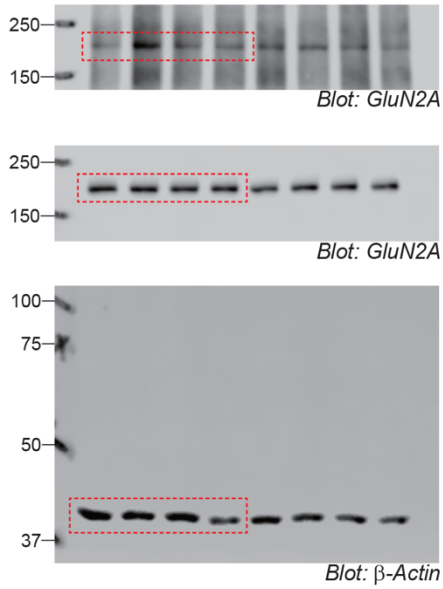

Figure 4c

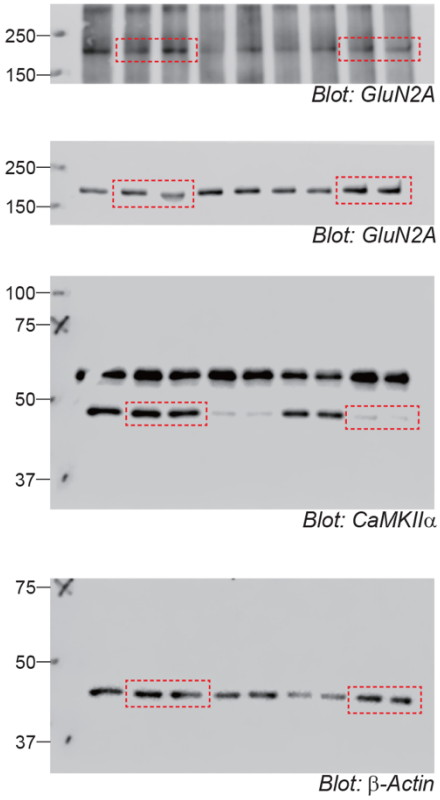

Figure 4e

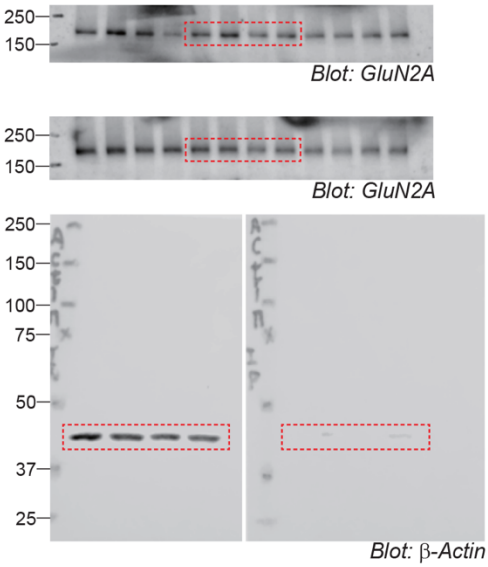

Data S3. Uncropped Images of Western Blots, Related to Figure 4.

Figure S1a

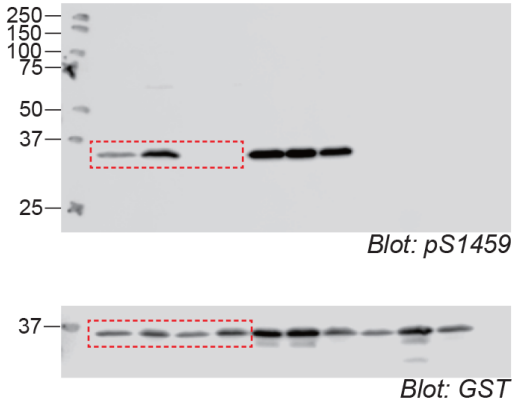

Figure S1c

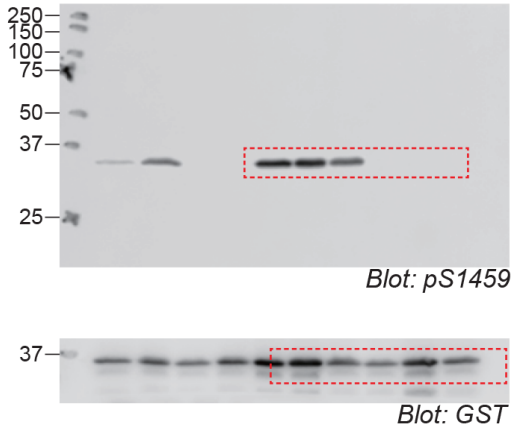

Data S4. Uncropped Images of Western Blots, Related to Figure S1.

Figure S2a

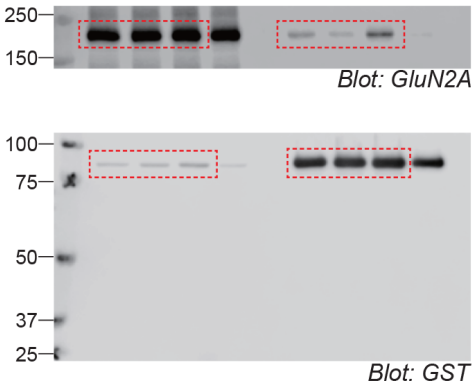

Figure S2c

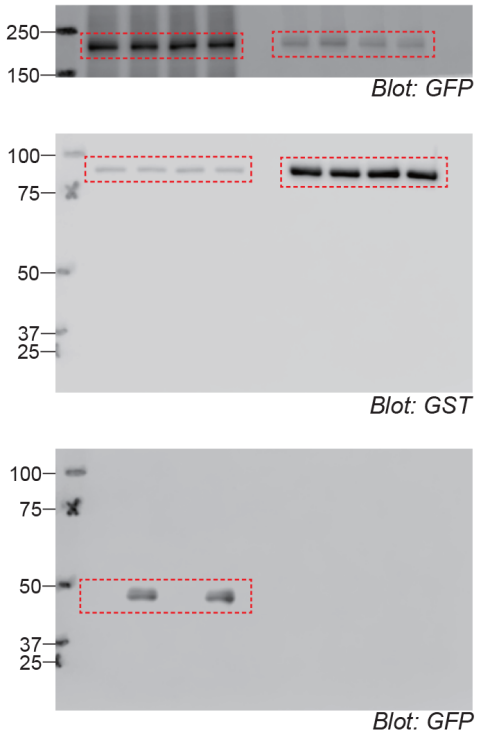

Data S5. Uncropped Images of Western Blots, Related to Figure S2.

Figure S3a

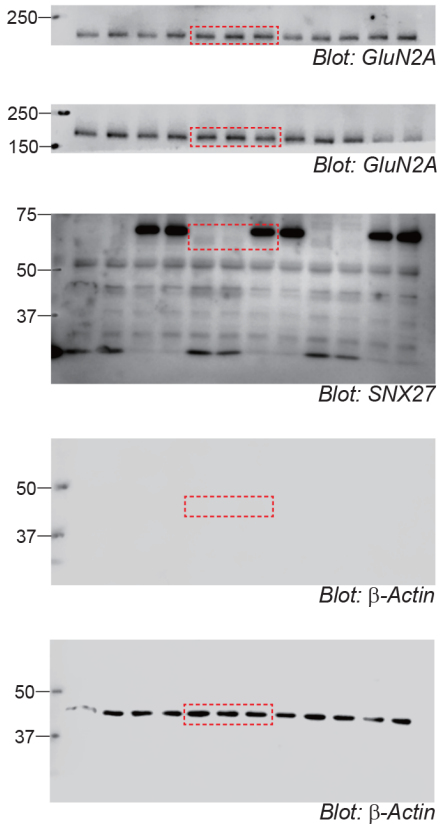

Data S6. Uncropped Images of Western Blots, Related to Figure S3.